Metabolomic Evaluation of Di-*n*-butyl Phthalate-Induced Teratogenesis in Mice

By: Hongfei Xia, Yi Chi, Xin Qi, Mingming Su, Yu Cao, Peipei Song, Xin Li, Tianlu Chen, Aihua Zhao, Yinan Zhang, Yi Cao, Xu Ma, and Wei Jia

Xia, H.F., Chi, Y., Qi, X. Su, M.M., Cao, Y., Song, P. P., Li, X., Chen, T.L., Zhao, A.H., Zhang. Y.N., Cao, Y., Ma, X., & Jia, W. (2011). Metabolomic evaluation of Di-n-Butyl Phthalate (DBP)-induced teratogenesis in mice. *Metabolomics, 7*(4), 559-571.

Abstract:

Di-*n*-butyl phthalate (DBP) has been linked to the neural, reproductive and developmental toxicity. We present here a metabolomic study that characterized the metabolic variations associated with the DBP-induced teratogenesis in maternal and fetal mice. DBP at 50 and 300 mg/kg were administrated to pregnant C57 mice, via gastric intubation on gestation day 7–9, respectively. Maternal mice were euthanized on gestation day 16 and examined for fetal development and malformations. Metabolomic study of maternal serum, placenta and fetal brain tissues was performed using gas chromatography time-of-flight mass spectrometry combined with multivariate data analysis (MVDA). The results showed that a 50 mg/kg dose of DBP had no significant effect on fetal development and a 300 mg/kg dose caused embryo resorption and fetal malformations (primarily eye abnormalities and encephalocele). MVDA indicated that DBP at two doses gave rise to disruption of maternal and fetal metabolic profiles characterized by significantly altered tricarboxylic acid cycle, amino acid, purine and lipid metabolism.

Article:

INTRODUCTION

Di-*n*-butyl phthalate (DBP) is a manufactured chemical commonly used as a plasticizer and additive in adhesives, printing inks, and hair spray products (Premysl et al. 2005). This odorless and colorless synthetic chemical can readily be released to the environment, due to its lack of covalent bonding to other matrix materials in products (Premysl et al. 2005). As a result, DBP has been detected in air, drinking water, soil and food products (ATSDR 1990; Chan and Meek 1994; IPCS 1997). Food is a primary source of human exposure to DBP and levels of DBP in food vary from 50 to 500 parts per billion (Kavlock et al. 2002). The acute toxicity of DBP is relatively low with oral LD_{50} values of 8–20 g/kg body weight in rats and 5–16 g/kg body weight in mice (IPCS 1997), however, long-term exposure to low doses of DBP in utero has been shown to induce serious impairment of the early reproductive (Foster et al. 2001; Gray et al. 1982; Wine et al. 1997) and neural development (Shiota et al. 1980; Shiota and Nishimura 1982) in animals. Other developmental anomalies such as delayed ossification, cleft palate and so on, have also been observed in low-dose DBP-treated animals (Shiota et al. 1980; Shiota and Nishimura 1982; Ema et al. 1993). Natural exposure to food and other materials containing

higher levels of DBP might potentially induce abnormal embryonic and fetal development and it has been reported that several phthalates, including DBP, detected in the urine of pregnant women were associated with genital defects in male infants (Swan et al. 2005).

Metabolomics or metabonomics, defined as the quantitative measurement of the dynamic multiparametric metabolic response of living systems to pathophysiological stimuli or genetic modification (Nicholson et al. 1999), has been extensively used in toxicological studies, clinical diagnosis, drug discovery, plant science and nutrition (Premysl et al. 2005; Weckwerth et al. 2004; Gibney et al. 2005; Um et al. 2009). Metabolomics focuses on endogenous low-molecular-weight metabolites (generally less than 1,000 Da) and attempts to capture changes in the metabolic network to reveal the essence of life activities. Currently, nuclear magnetic resonance (NMR) and hyphenated chromatography/mass spectrometry (MS) such as gas chromatography or liquid chromatography coupled with mass spectrometry (GC-MS or LC-MS) (Chen et al. 2006; Sugimoto et al. 2005; Wang et al. 2007) are the analytical platforms routinely used in metabolomic studies.

The use of DBP is restricted or banned in cosmetics and toys in Western countries, however, comprehensive understanding of DBP-induced toxicity is still lacking. We therefore present a pilot study on neural and embryonic toxicity of DBP in a pregnant mouse model of intrauterine exposure with DBP using a metabolomics approach. Sera, placentas, and fetal brain tissues were collected from low- and high-dose DBP-treated mice as well as healthy controls. The global changes of metabolites in these biological matrixes of DBP-treated mice were obtained using a hyphenated gas chromatography/time-of-flight mass spectrometry (GC/TOFMS) in conjunction with multivariate data analysis (MVDA). The study identified a number of differentially expressed metabolites in association with the teratogenic toxicity of DBP. These metabolite markers collectively revealed the DBP-induced global metabolic alterations and provided mechanistic insights into the metabolic pathway alterations, along with neurodevelopmental abnormalities resulting from DBP exposure.

EXPERIMENTAL METHODS

Animal handling and sampling

The animal study was approved by the Ethics Committee of National Research Institute for Family Planning (Beijing, P. R. China). Sexually mature, healthy female C57 mice (weighing 18–22 g) were purchased from and raised in the Laboratory Animal Center, the Academy of Military Medical Sciences, Chinese Academy of Sciences (Beijing, P. R. China). The mice were housed under a controlled condition of 12 h light/12 h dark cycle at approximately 22–24°C with a relative humidity of 60–70%. The mice had free access to chow and water ad libitum. Each female mouse was mated with a sex ratio 3:1 (female:male), and gestation day (gd) 0 was defined by the presence of a vaginal plug or a sperm positive vaginal smear. In our preliminary experiments, the pregnant mice (n = 5 per group) were given 50, 300, 1,000 and 2,250 mg/kg DBP in olive oil (Sigma, St. Louis, MO) on gd. 7, but none of the fetuses showed apparent external malformations with the exception of embryo growth retardation in the 2,250 mg/kg DBP group. However, all of the embryos were absorbed at doses of 750 and 1,000 mg/kg DBP (n = 5 per group) on gd. 7–9. Based on these preliminary results, the pregnant mice were randomly divided into three groups: two model groups with a daily dose of DBP at 50 mg/kg body weight (n = 12, labeled as low-dose group) and 300 mg/kg (n = 12, labeled as high-dose group) by

gastric intubation on gd. 7–9, respectively, and a control group (n = 12) dosed with olive oil. Only seven mice from each group were used to provide samples for metabolomics study.

All the mice were euthanized by intraperitoneal injection of pentobarbital (50 mg/kg body weight) at the 16th day of gestation. The blood samples were collected by enucleation of eyeball and the resulting sera were stored at −80°C until analysis. Placenta weight, number of implantation sites per litter, number of fetal resorptions per litter and number of live and dead fetuses per litter were recorded. The percentage of post-implantation loss per litter, live and dead fetuses per litter, and fetal resorptions per litter were calculated accordingly. Live fetuses and their brains, hearts, and livers were also weighed. All of the organs of live fetuses were examined for external abnormalities. All the brain or placenta tissue samples per litter were mixed as a single sample and stored at −80°C for metabolomic analysis.

Serum sample extraction

The extraction of serum metabolites was performed following our previously published procedures (Qiu et al. 2009). Briefly, each 100- µl aliquot of serum sample was added into a 1.5-ml microcentrifuge tube. Each 10 µl of internal standards, including L-2-chlorophenylalanine and heptadecoic acid, were added to monitor the batch reproducibility. The tube was vortexed for 10 s and 300 µl of a mixture of chloroform and methanol (1:3, v/v) was added for metabolite extraction. The resulting mixture was vortexed for 30 s and centrifuged at 10, 000 rpm for 10 min. Each 300-µl supernatant was diverted to a glass vial for further derivatization.

Tissue sample extraction

Tissue samples (fetal brains and placentas) were extracted using our two-step extraction method with minor modifications (Pan et al. 2010). Internal standards, including L-2-chlorophenylalanine and heptadecoic acid, were also added to monitor the batch reproducibility. Specifically, each 100 mg of tissue sample was homogenized and extracted with 500-µl solvent of chloroform/methanol/water (1:2:1, v/v/v). The resulting mixture was centrifuged at 10, 000 rpm for 10 min. A 150-µl supernatant was transferred into a glass vial and the pellet was re-extracted using 500 µl of methanol. Another 150-µl supernatant was obtained and the two supernatants were combined for the following derivatization.

Chemical derivatization prior to GC/TOFMS Analysis

Each 300 µl of the resulting serum or tissue extracts was dried under vacuum and reconstituted in 80 µl of methoxylamine hydrochloride (15 mg/ml in pyridine) for 90 min at 30°C. The mixture was silylated with 80 µl of *N*,*O*-bis-trimethylsilyl-trifluoroacetamide (BSTFA) (containing 1% trimethylchlorosilane) (Sigma, St. Louis, MO) for 1 h at 70°C. The product was vortexed for 10 s and kept at room temperature for 1 h. Each 1-µl aliquot of the derivatized product was injected at a splitless mode into an Agilent 6890N GC system coupled with a Pegasus HT TOFMS (Leco, St. Joseph, MI). A DB-5MS capillary column coated with 5% Diphenyl cross-linked 95% dimethylpolysiloxane (30 m × 250 µm i.d., 0.25-µm film thickness; Agilent J&W Scientific, Folsom, CA) was used. The temperature of injector, transfer line, and the ion source were set to 270, 260, and 200°C, respectively. Helium was used as the carrier gas at a constant flow rate of 1 ml/min. The initial oven temperature was set at 80°C for 2 min and raised up to 180°C with a rate of 10°C/min, to 230°C with a rate of 6°C/min, to 295°C with a

rate of 40°C/min, and finally held at 295°C for 7 min. The measurements were made with electron impact ionization (70 eV) in the full scan mode (*m/z* 30–600).

Data processing

The observational data obtained from animal examinations was analyzed by one-way analysis of variance (ANOVA) with LSD test in SPSS 13 statistical software package (The SPSS Inc., Chicago, IL). A threshold of P value <0.05 was considered statistically significant.

The GC/TOFMS data files were processed following our previously published procedures (Wang et al. 2007). The resulting data set was normalized, mean-centered, and uv-scaled (unit variance scaling) before multivariate statistical analysis (SIMCA-P 12.0.1, Umetrics, Umeå, Sweden). Principal component analysis (PCA) was initially utilized to visualize general clustering trends of the three groups. Based on the PCA scores plot, metabolic profiles from DBP-treated groups were distinct from the control group; however, PCA could not depict a clear separation between high-dose and low-dose groups (figure not shown). In this case, we used a supervised classification method partial least square- discriminant analysis (PLS-DA) to visualize the different metabolic profiles among the three groups. Furthermore, to identify the differential metabolites between each DBP-treated group versus the control group, a more sophisticated mathematical method, orthogonal partial least square-discriminant analysis (OPLS-DA) was used by filtering the unrelated information from the systematic variations. Specially, the OPLS-DA technique (Bylesjo et al. 2006), a modification of the PLS-DA method, is able to divide the systematic variation of **X** matrix (herein, raw GC/TOFMS data set) into two parts: one that is linearly correlated/predictive to **Y** (herein, group descriptors, i.e., control group, low-dose group, and high-dose group) and one that is orthogonal to **Y**. The predictive variation of **Y** in **X** is modeled by the predictive components only and a single predictive component is necessary for two-group classification. Therefore, the OPLS-DA method provides improved model transparency and interpretability without compromising the power of the model prediction. For PLS-DA and OPLS-DA modeling in SIMCA-P software, the default sevenfold cross-validation procedure was carried out to avoid model overfitting and two fundamental parameters R^2Y and Q^2Y were attained accordingly. The values of R^2Y and Q^2Y approaching 1.0 indicate a reliable model with satisfactory predictability and the value of $Q^2Y_{cum} \geq 0.4$ is considered a reliable model (www.umetrics.com). The detected metabolites with variable importance on project (VIP) greater than 1.0 were considered meaningful in this study (Ni et al. 2008; Qiu et al. 2010). Additionally, a non-parametric univariate Mann–Whitney test was used to verify whether the results obtained from multivariate statistics were also significant at a univariate level. The critical *p*-value of the test was set as 0.05 in this study.

Metabolite identification

We were able to identify a wide range of endogenous metabolites by comparing the spectra with those in NIST/EPA/NIH (NIST 05) mass spectral library (National Institute of Standards and Technology, Gaithersburg, MD). Subsequently, those metabolites were further verified by our in-house mass spectral library that was established with available reference compounds.

RESULTS AND DISCUSSION

General information about the animal experiment

The effects of DBP on dams and embryos are shown in Table 1. In the high-dose group, there was a significant reduction ($P < 0.01$) in the number of live fetuses, together with a significant increase ($P < 0.01$) in fetal resorptions. The percentage of post-implantation loss per litter markedly increased to 27.48%, whereas the percentage of live fetuses per litter markedly decreased to 71.45%. Placenta weight was significantly reduced in high-dose groups ($P < 0.01$) as compared to the control group.

Table 1: Reproductive and fetal parameters in mice treated with DBP

	Dose (mg/kg/day)		
	0	**50**	**300**
No. of pregnant rats	12	12	12
No. of implantation sites/litter	7.08 ± 0.56	7.50 ± 0.26	7.46 ± 0.49
No. of resorptions/litter	0.46 ± 0.22	0.58 ± 0.26	2.05 ± 0.44**
No. of dead fetuses/litter	0.00 ± 0.00	0.00 ± 0.00	0.08 ± 0.08
No. of live fetuses/litter	6.62 ± 0.49	6.92 ± 0.38	5.33 ± 0.57**
Percentage of post-implantation loss/litter	6.50	7.73	27.48
Percentage of dead fetuses/litter	0	0	1.07
Percentage of resorptions/litter	6.50	7.73	28.55
Percentage of live fetuses/litter	93.50	92.27	71.45
Placenta weight (g)	0.1188 ± 0.0047	0.1134 ± 0.0020	0.0966 ± 0.0027**

Data are presenting as mean ± SD. ** $P < 0.01$ (one-way ANOVA)

Table 2 also demonstrates that the weight of fetuses, fetal liver, brain and heart were significantly reduced in high-dose group. These were also decreased in low-dose group, but not significantly. No fetal malformations were observed in the low-dose group (Table 3). The overall percentage of fetuses with malformations was 25% of total live fetuses in the high-dose group and a variety of external malformations were observed in half of this group's 12 litters (Table 3). The primary malformations were eye abnormalities and encephalocele. The corresponding histopathological images are provided in Fig. 1.

Table 2: The effects of DBP on fetal development

	Dose (mg/kg/day)		
	0	**50**	**300**
No. of fetuses	41	40	40
Fetal body weight (g)	0.4562 ± 0.0134	0.4307 ± 0.0119	0.3615 ± 0.0158**
Fetal brain weight (g)	0.0448 ± 0.0021	0.0407 ± 0.0016	0.0384 ± 0.0012*
Fetal heart weight (g)	0.0059 ± 0.0006	0.0058 ± 0.0004	0.0047 ± 0.0004*
Fetal liver weight (g)	0.0510 ± 0.0055	0.0470 ± 0.0022	0.0393 ± 0.0030**

Data are presenting as mean ± SD. * $P < 0.05$, ** $P < 0.01$ (one-way ANOVA)

Table 3: Examination for malformations

	Dose (mg/kg/day)		
	0	**50**	**300**
Total number of fetuses (litters) examined	84 (12)	83 (12)	64 (12)
Encephalocele	0	0	3
Exencephaly	0	0	0
Taillessness	0	0	1
Eye agenesis (anophthalmos, microphthalmos or eye abnormality)	0	0	16
Short limbs	0	0	1
Complicated with multiple malformations			
Eye agenesis and short limbs	0	0	0
Eye agenesis and taillessness	0	0	0
Eye agenesis and Encephalocele	0	0	3
Eye agenesis, taillessness and short limbs	0	0	1
Eye agenesis, taillessness, short limbs and Encephalocele	0	0	0
Total number of fetuses (%) with malformations	0	0	16 (25.00%)
Total number of litters (%) with external malformations	0	0	6 (50.00%)

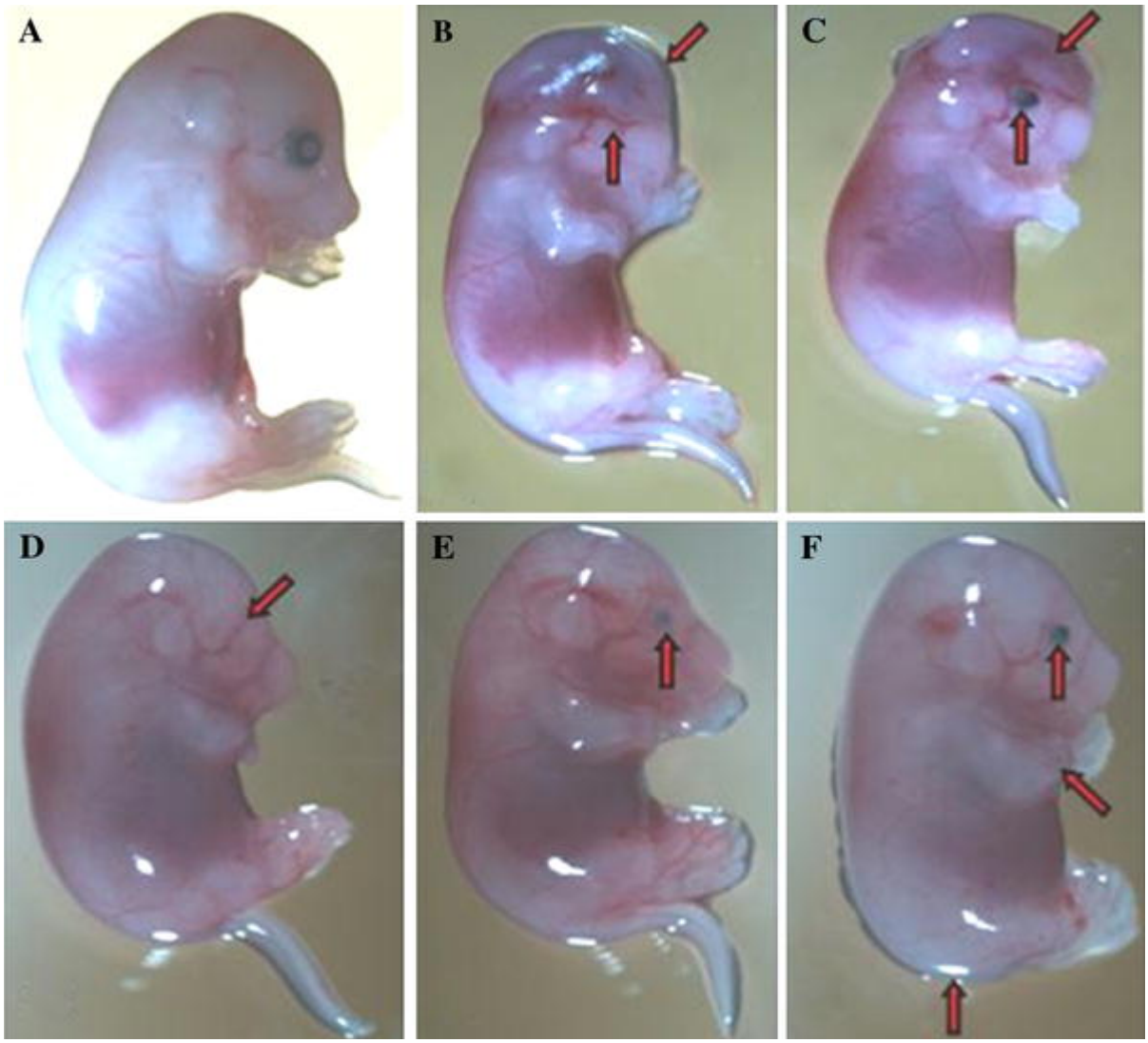

Figure 1: Representative images of histopathological examinations on fetuses. **a** Normal fetal mouse. **b** Fetus with encephalocele and anopia. **c** Encephalocele and eye abnormities. **d** Anopia. **e** Eye abnormities. **f** Eye abnormities and anury

Metabolic variation caused by DBP exposure

Using a GC/TOFMS-based metabolomics approach, we were able to detect 373, 473 and 407 chromatographic peaks from the total ion current (TIC) chromatograms of serum, placenta and fetal brain tissue, respectively. Each representative TIC chromatogram of serum, placenta, or fetal brain tissue from the control group was provided in Fig. 2a–c. As also illustrated in the Fig. 2d–f, there is a distinct separation between the control and DBP treatment groups, and a separation between the two treatment groups, as visualized in the three-dimensional PLS-DA scores plot. Additionally, a more distinct separation between the metabolomic profile of each treatment group versus the control group was observed in the OPLS-DA score plot generated from serum, placenta, or fetal brain tissue (Fig. 3a–f). The modeling parameters of these models were presented in Table 4. Based on the threshold of VIP values (VIP > 1), the differentially expressed metabolites in each type of biological matrix are listed in Tables 5 and 6.

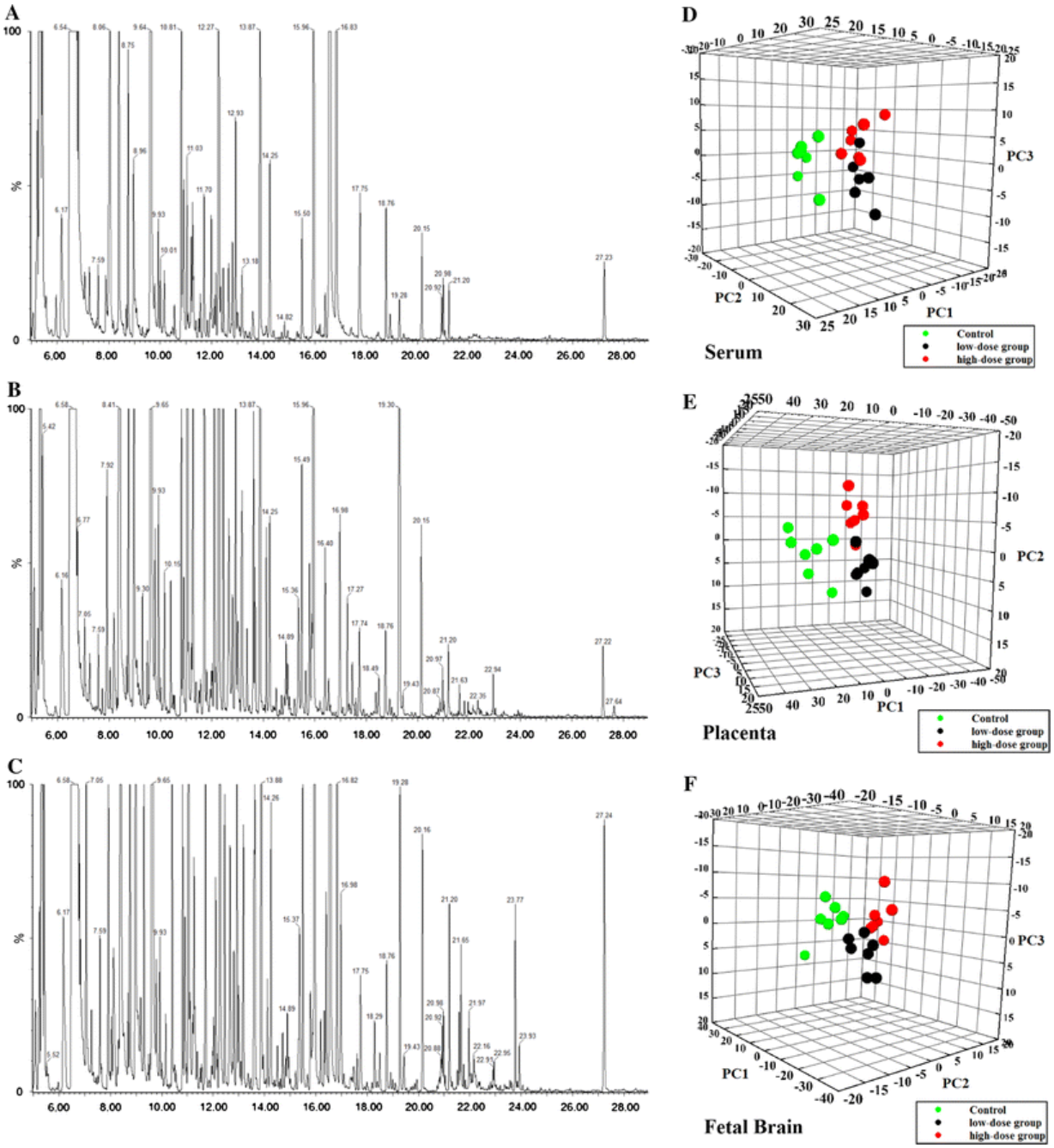

Figure 2: Representative TIC chromatograms of the three types of samples. **a** Serum. **b** Placenta. **c** Fetal brain tissue. Based on the retention times, the differential metabolites between each of DBP-treated groups versus the control group in Tables 5 and 6 can be retrieved from these representative chromatograms. Three-dimensional scores plot obtained from PLS-DA of global metabolites in the different types of samples among the three groups. **d** Serum. **e** Placenta. **f** Fetal brain tissue. Distinct metabolic profiles between DBP-dosed groups and control can be attained readily in the first PLS-DA component, and separate trend can also be observed between the two DBP-treated groups in different PLS-DA components

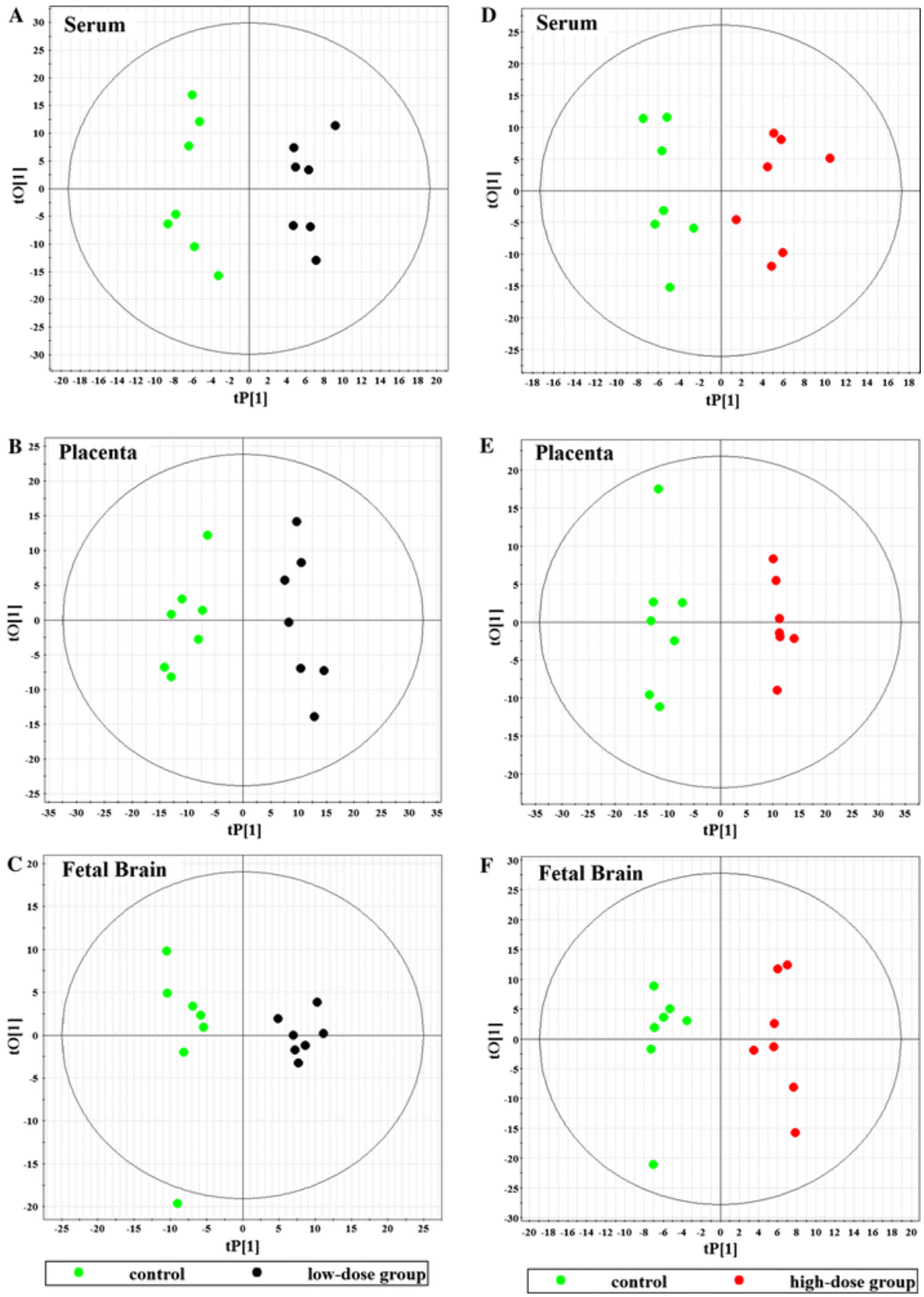

Figure 3: OPLS-DA scores plots (tP[1]/tO[1]) showing a distinct separation between each of the DBP-treated group versus the control group according to the metabolites from serum (**a** low-dose group, **b** high-dose group), placenta (**c** low-dose group, **d** high-dose group), and fetal brain tissue (**e** low-dose group, **f** high-dose group)

Table 4: The parameters for PLS-DA and OPLS-DA models in this study

Group (n = 7 per group)	Type	Serum				Placenta				Fetal brain tissue			
		No.[a]	R^2X_{cum}[b]	R^2Y_{cum}[c]	Q^2Y_{cum}[d]	No.	R^2X_{cum}	R^2Y_{cum}	Q^2Y_{cum}	No.	R^2X_{cum}	R^2Y_{cum}	Q^2Y_{cum}
High-, low-dose DBP & control	PLS-DA	6	0.76	0.93	0.49	5	0.70	0.96	0.68	7	0.80	0.97	0.55
Low-dose vs. control	OPLS-DA	1P+1O	0.47	0.94	0.57	1P+1O	0.50	0.94	0.76	1P+2O	0.56	0.95	0.67
High-dose vs. control	OPLS-DA	1P+1O	0.42	0.88	0.42	1P+1O	0.49	0.98	0.86	1P+2O	0.63	0.96	0.56

[a]Components required for a valid model and prediction. For OPLS-DA, *P* predictive component, *O* orthogonal component. More details refer to the text. [b] R^2X_{cum}, the cumulative sum of squares (SS) of the entire **X** explained by all extracted components. [c] R^2Y_{cum}, the cumulative SS of all the *y*-variables explained by the extracted components. [d] Q^2Y_{cum}, the cumulative Q^2 for all the *x*-variables (PC) and *y*-variables (PLS) for the extracted components. The values of R^2Y and Q^2Y approaching 1.0 indicate a perfect model with a satisfactory predictive ability (cross-validation) and the value of $Q^2Y_{cum} \geq 0.4$ is considered a reliable model

Table 5: Differentially expressed metabolites in high-dose group versus control group

No.	RT/min	Metabolite	Metabolic pathway	Serum			Placenta			Fetal brain tissue		
				VIP[b]	FC[c]	*P* [d]	VIP	FC	*P*	VIP	FC	*P*
1	7.35	2-Oxo-3-methylvalerate	Amino acid metabolism	1.7	−1.8	0.0641	/	/	/	/	/	/
2	7.59	Valine[a]	Amino acid metabolism	1.5	−1.6	0.1320	0.2	1.2	0.5270	1.1	−1.4	0.2770
3	8.68	Isoleucine[a]	Amino acid metabolism	1.8	−1.8	0.0489	0.2	1.3	0.4010	1.3	−1.5	0.2010
4	8.87	Glycine	Amino acid metabolism	/	/	/	/	/	/	0.9	−1.3	0.4060
5	11.04	Aminomalonate	Amino acid metabolism	1.2	−1.3	0.3540	0.7	−1.2	0.4940	0.6	1.3	0.4060
6	11.70	Pyroglutamate[a]	Amino acid metabolism	/	/	/	/	/	/	1.5	2.2	0.0130
7	11.80	γ-Aminobutyric acid	Amino acid metabolism	/	/	/	/	/	/	0.4	−1.2	0.4820
8	12.10	Creatinine[a]	Amino acid metabolism	0.7	−1.3	0.4180	1.6	2.2	0.0063	1.8	−2.0	0.0210
9	12.90	Glutamate[a]	Amino acid metabolism	/	/	/	0.1	1.2	0.6000	1.3	−1.3	0.3370
10	5.19	Pyruvate[a]	Carbohydrate Metabolism	0.2	−1.0	0.9540	1.3	1.9	0.0238	1.5	1.7	0.0850
11	5.34	Lactate	Carbohydrate Metabolism	1.3	1.4	0.2030	1.3	2.2	0.0087	1.5	−2.0	0.0210
12	5.74	Glycolate	Carbohydrate Metabolism	1.3	1.4	0.2240	1.2	1.8	0.0460	1.3	−1.7	0.0850
13	14.2	Ribitol[a]	Carbohydrate Metabolism	2	1.8	0.0372	0.9	1.5	0.1720	/	/	/
14	14.71	Glycerol 3-phosphate[a]	Carbohydrate Metabolism	1.2	1.4	0.2470	/	/	/	1.4	1.7	0.0850
15	16.20	Fructose[a]	Carbohydrate Metabolism	2.0	2.0	0.0206	0.6	1.3	0.2940	/	/	/
16	17.09	D-sorbitol[a]	Carbohydrate Metabolism	/	/	/	1.5	2.0	0.0157	/	/	/
17	17.48	Gluconate	Carbohydrate Metabolism	1.7	−1.6	0.1050	1	1.6	0.1140	1.4	−1.8	0.0640
18	19.30	Myo-inositol[a]	Carbohydrate Metabolism	0.8	−1.2	0.4880	1.5	2.2	0.0087	0.7	−1.3	0.3380
19	9.49	Fumarate[a]	TCA cycle	2.2	−2.0	0.0279	0.6	1.3	0.2940	1.0	1.4	0.3060
20	11.26	Malate	TCA cycle	2.0	−2.1	0.0151	0	−1.1	0.7130	0.8	1.4	0.2250
21	14.57	*cis*-aconitic acid[a]	TCA cycle	/	/	/	/	/	/	1.3	−2.1	0.0181
22	20.98	Oleate[a]	Lipid metabolism	1.6	−1.5	0.1640	1.3	1.9	0.0274	0.2	1.4	0.2250
23	21.20	Stearate[a]	Lipid metabolism	1.2	1.3	0.3540	1.6	2.2	0.0063	0.6	0.8	0.5650
24	21.97	Arachidonate[a]	Lipid metabolism	1.3	1.4	0.2470	1.1	1.7	0.0742	0	−1.1	0.7490
25	22.32	4-Aminohippurate[a]	Lipid metabolism	/	/	/	2	−2.7	0.0011	/	/	/
26	22.96	*cis*-5,8,11,14,17-	Lipid metabolism	/	/	/	1.7	2.6	0.0016	/	/	/

		eicosapentaenoic acid										
27	23.72	1-(9z-Octadecenoyl)-glycerol	Lipid metabolism	2.5	−2.3	0.0077	/	/	/	/	/	/
28	23.92	2-(9z-Octadecenoyl)-glycerol	Lipid metabolism	2.3	−2.2	0.0128	/	/	/	/	/	/
29	24.06	1-Stearoyl-glycerol[a]	Lipid metabolism	2.4	2.3	0.0055	1.6	2.3	0.0046	0.8	1.5	0.1800
30	8.13	Urea[a]	Purine degration	/	/	/	1.2	2.0	0.0155	/	/	/
31	11.83	Allantoin[a]	Purine degration	/	/	/	1.4	2.0	0.0156	/	/	/
32	18.29	Xanthine[a]	Purine degration	2.5	2.1	0.0109	1.6	2.3	0.0046	1.3	1.4	0.1590
33	22.32	Uridine[a]	Primidine metabolism	/	/	/	1.3	2.0	0.0180	0.4	1.1	0.7490

[a]Those metabolites were verified by reference compounds available in our laboratory and the remaining metabolites were identified using commercial library database NIST05. [b] Variable importance in projection (VIP) was obtained from OPLS-DA Model. [c] Fold change (FC) and *P* values were calculated by Wilcoxon–Mann–Whitney Test. A positive FC value means that concentration of the metabolite is relatively higher in DBP-treated group, while a negative value suggests a relatively lower concentration in the DBP group as compared to the controls. "/" represents the metabolite is not detected in the biological matrix

Table 6: Differentially expressed metabolites in low-dose group versus control group

No.	RT/min	Metabolite	Metabolic pathway	Serum			Placenta			Fetal brain tissue		
				VIP[b]	FC[c]	*P* [d]	VIP	FC	*P*	VIP	FC	*P*
1	7.59	Valine[a]	Amino acid metabolism	2.1	−2.0	0.0209	0.6	−1.2	0.4620	1.3	−2.0	0.0212
2	8.68	Isoleucine[a]	Amino acid metabolism	2.5	−2.2	0.0073	0.6	−1.3	0.3450	0.6	1.1	0.8480
3	8.87	Glycine[a]	Amino acid metabolism	/	/	/	/	/	/	1.4	−2.6	0.0027
4	11.04	Aminomalonate	Amino acid metabolism	2.1	−2.0	0.0157	0.4	−1.1	0.7930	0.8	1.2	0.4820
5	11.70	Pyroglutamate[a]	Amino acid metabolism	/	/	/	/	/	/	1.2	2.1	0.0181
6	11.80	γ-Aminobutyric acid	Amino acid metabolism	/	/	/	/	/	/	1.3	−2.1	0.0181
7	12.10	Creatinine[a]	Amino acid metabolism	1.4	−1.7	0.0517	1.2	1.7	0.0590	1.2	−1.9	0.0331
8	12.90	Glutamate[a]	Amino acid metabolism	/	/	/	0.5	−1.3	0.3450	1.7	−2.5	0.0040
9	5.34	Lactate	Carbohydrate Metabolism	0.2	1.1	0.7130	1.4	2.1	0.0120	1.7	−1.9	0.0350
10	5.74	Glycolate	Carbohydrate Metabolism	2.4	2.2	0.0070	1.4	2.0	0.0160	1.9	−2.5	0.0040
11	14.20	Ribitol[a]	Carbohydrate Metabolism	2.2	2.0	0.0160	1.4	2.0	0.0160	/	/	/
12	14.71	Glycerol 3-phosphate[a]	Carbohydrate Metabolism	1.2	1.5	0.1720	/	/	/	0.3	−1.2	0.5650
13	17.09	D-Sorbitol[a]	Carbohydrate Metabolism	/	/	/	1.5	2.0	0.0160	/	/	/
14	17.48	Gluconate	Carbohydrate Metabolism	1.7	−1.7	0.0660	1.5	2.1	0.0100	1.4	−2.5	0.0040
15	19.30	Myo-inositol[a]	Carbohydrate Metabolism	1.6	−1.4	0.2270	1.6	2.2	0.0060	0.6	−1.4	0.2250
16	9.49	Fumarate[a]	TCA cycle	1.7	−1.6	0.1150	0.2	1.0	0.9160	0.3	−1.1	0.7010
17	11.26	Malate	TCA cycle	1.8	−1.8	0.0460	0.6	−1.4	0.2480	1.4	2.0	0.0300
18	14.57	*cis*-aconitic acid[a]	TCA cycle	/	/	/	/	/	/	1.4	−2.1	0.0180
19	20.98	Oleate[a]	Lipid metabolism	1.0	−1.3	0.3710	1.4	1.8	0.0356	0.3	1.5	0.1800
20	21.20	Stearate[a]	Lipid metabolism	1.5	1.5	0.1720	1.4	2.1	0.0100	0.1	−1.3	0.4420
21	21.97	Arachidonate[a]	Lipid metabolism	1.6	1.9	0.0274	1.1	1.7	0.0585	0.2	−1.3	0.3700
22	22.32	4-Aminohippurate[a]	Lipid metabolism	/	/	/	1.6	−2.2	0.0086	/	/	/
23	22.96	*cis*-5,8,11,14,17-eicosapentaenoic acid	Lipid metabolism	/	/	/	1.6	2.4	0.0033	/	/	/
24	23.72	1-(9z-octadecenoyl)-glycerol	Lipid metabolism	2.1	−2.0	0.0157	/	/	/	/	/	/
25	23.92	2-(9z-octadecenoyl)-glycerol	Lipid metabolism	2.8	−2.4	0.0033	/	/	/	/	/	/
26	24.06	1-Stearoyl-glycerol[a]	Lipid metabolism	2.2	2.1	0.0135	1.0	1.7	0.0585	0.3	1.2	0.5650
27	8.13	Urea[a]	Purine degration	/	/	/	1.2	2.0	0.0155	/	/	/
28	15.37	Hypoxanthine[a]	Purine degration	/	/	/	/	/	/	1.1	1.8	0.0460
29	18.29	Xanthine[a]	Purine degration	2.2	2.0	0.0160	1.3	1.9	0.0274	1.1	1.6	0.1100
30	22.32	Uridine[a]	Primidine metabolism	/	/	/	1.1	1.8	0.0357	1.3	2.0	0.0300

[a]Those metabolites were verified by reference compounds available in our laboratory and the remaining metabolites were identified using commercial library database NIST05. [b] variable importance in projection (VIP) was obtained from OPLS-DA Model. [c] Fold change (FC) and *p* values were calculated by Wilcoxon–Mann–Whitney test. A positive FC value means that concentration of the metabolite is relatively higher in DBP-treated group, while a negative value suggests a relatively lower concentration in the DBP group as compared to the controls. "/" represents the metabolite is not detected in the biological matrix

Interpretation of metabolic variations

In our study, pregnant mice were administrated with DBP on gd. 7–9, which is the critical period of neural tube formation and closure, and optic vesicle formation (DeSesso et al. 1999). It appeared that the primary abnormalities in the experimental model groups are eye agenesis and encephalocele, which is consistent with the observed adverse effects on neural tube development due to exposure to exogenous toxicants in this special period of fetal development (DeSesso et al. 1999). Short limbs and taillessness were also observed as well as combination of these malformations.

Maternal blood is the main source for fetal nutrition and the placenta is the compartment where the fetus exchanges nutrients and metabolites with the mother. In addition, the brain is the major site of embryo malformation due to DBP exposure in our study. Metabolite profiling of these three biological compartments can help elucidate the complex process of neural developmental abnormality through changes in metabolite expression and flux. In this study, we observed a distinct alteration of metabolite profiles in mice exposed to DBP in both dams and fetuses. The most significantly perturbed metabolic pathways include carbohydrate, amino acid, lipid, and purine metabolism, as illustrated in Fig. 4.

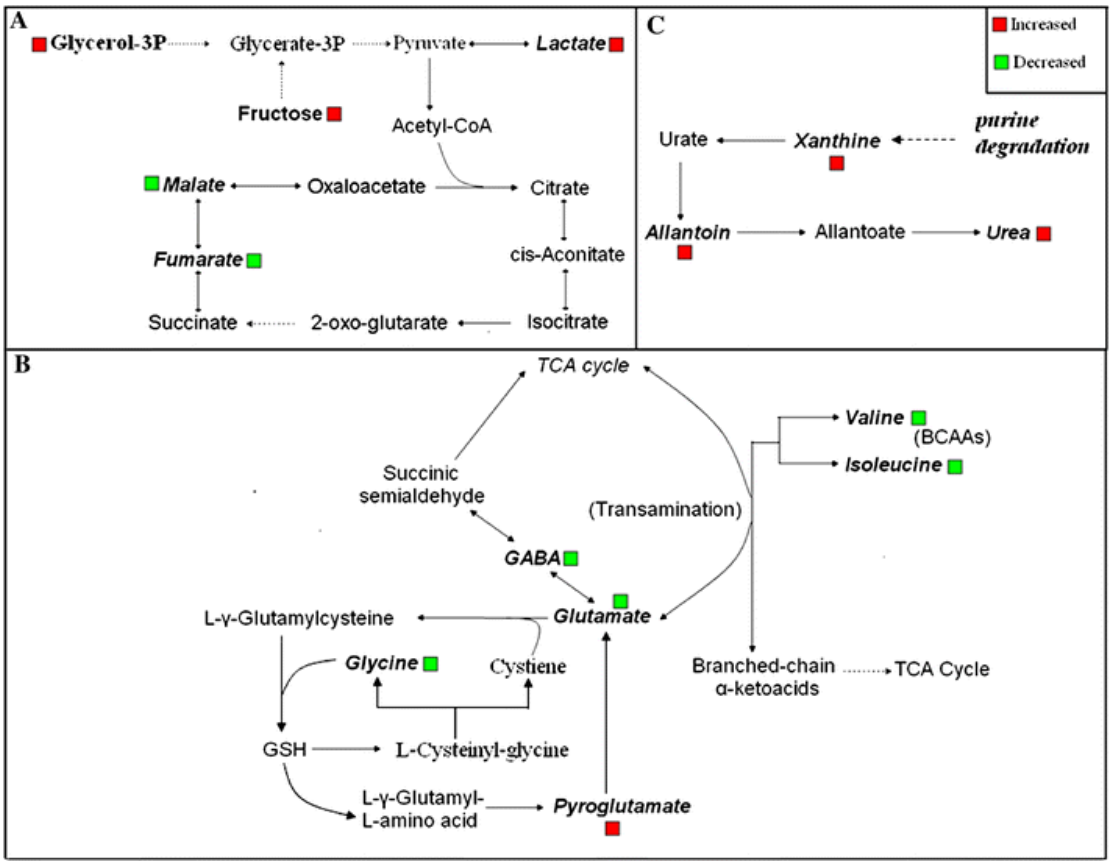

Figure 4: The altered metabolic pathways in response to the DBP exposure. **a** TCA cycle and glycolysis. **b** Glutamate-related metabolism. **c** Purine degradation. Metabolites detected in this study are highlighted with *grey/black color* in bond *italic font*. More details refer to the text and Tables 5 and 6

In this study, the metabolic profiles of both low and high dose DBP-treated pregnant rats and their fetal brain tissues are distinct from those of the controls. Significant alterations in serum metabolites directly reflect DBP's impact on the pregnant rats and these metabolic alterations will subsequently impact the placental and fetal development. As seen in Table 1, the weight of the placentas in the high-dose group significantly decreased. Fumarate and malate are downstream metabolites of succinate in the TCA cycle (Krebs 1957). The significantly decreased levels of fumarate and malate in serum could be associated with mitochondrial toxicity of DBP due to the fact that DBP is a strong inhibitor of succinic dehydrogenase (Tanaka et al. 1978; Melnick and Schiller 1982). As the TCA cycle was inhibited in DBP-treated rats, anaerobic glycolysis could have been activated for an alternative energy supply; with the expected result of an enhanced level of lactate, fructose and glycerol 3-phosphate, as observed in Tables 5 and 6. Since anaerobic glycolysis and TCA cycle are the critical metabolic pathways for mitochondrial respiration (Fernie et al. 2004), the disturbance of these essential metabolites suggests an impaired mitochondrial respiration in DBP groups. Mitochondria are central to energy metabolism and cellular signaling and play fundamental roles in synthesis of nucleotides, active transport processes, cell motility, and cell proliferation (Rustin 2002). It has been recently reported that exposure to pesticide would increase the risk of Neural tube defects due to that many pesticides can inhibit mitochondrial oxidative phosphorylation (Rull et al. 2006). In this case, DBP could also cause a defective mitochondrial energy production during the process of fetus formation and development.

Several important amino acids were altered in serum or fetal brain tissue, including isoleucine and its' degradation product, 2-oxo-3-methylvalerate, and valine which decreased in the DBP-treated pregnant rats. Isoleucine and valine belongs to essential branched-chain amino acids (BCAAs) that are able to convert into branched-chain α-keto acids coupled with the production of glutamate from α-ketoglutarate through branched-chain aminotransferase (BCAT) (Yudkoff 1997). Since cytosolic BCAT (BCATc, one isoform of BCAT) mRNA, is strongly expressed in developing mouse brains (Castellano et al. 2007), the depletion of BCAAs in maternal sera may result in decreased BCAAs in fetuses and then may negatively impact the neurodevelopmental process as an insufficient nitrogen source for the synthesis of neurotransmitter glutamate. In fetal brain tissues, we observed significantly decreased level of valine, glutamate and γ-amino-*n*-butyric acid (GABA) that are principal neurotransmitters of developmental signals in neural tube formation, and neuronal and glial differentiation (Lauder 1983) in low-dose group. These three metabolites were also reduced in high-dose group, though not significantly. The depleted level of glutamate and GABA in the fetal brain tissues may be strongly related to the down-regulation of BCAAs in the sera of their mothers.

Glycine can generate glutathione (GSH), which will in turn, produce pyroglutamate in the γ-glutamyl cycle (Meister 1974, 1995). GSH is an important intracellular antioxidant that protects against a variety of different oxidants. Increased pyroglutamate and decreased glycine were observed in the fetal brain tissue of DBP-treated groups which indicates that DBP exposure may induce GSH disruption. A previous study also reported that DBP can affect the antioxidant system of the organism and inhibit the activity of superoxide dismutase (Prasanth et al. 2009). We speculated that DBP could disrupt antioxidant system and may cause oxidative stress. Since DBP could cross the placental and fetal barrier (Saillenfait et al. 1998), the antioxidant system of

fetuses may be disturbed by DBP that would be harmful to fetal development. Numerous reports suggested free radical-mediated mechanism of xenobiotics-induced abnormal embryonic development(DeSesso et al. 1999; Kotch et al. 1995; Dean et al. 2002).

In the placentas of the DBP-treated groups, a series of metabolites of purine catabolism, such as xanthine, allantoin and urea significantly elevated (Tables 5, 6). The increased levels of these metabolites, together with the elevation of uridine, suggest an activation of nucleic acid degradation. DBP could give rise to DNA damage (Wellejus et al. 2002). Thus, the upregulation of metabolites mentioned above may be related to DNA damage caused by DBP. Superoxide anions are generated during the conversion of xanthine into uric acid, and that this reaction will aggravate lesions in the nucleic acid (Pippenger 2003).

We also observed perturbations in lipid metabolism both in dam and fetus. Wyde et al. reported that DBP may affect lipid homeostasis (Bell 1982; Wyde et al. 2005). We observed significantly decreased oleate, stearate, arachidonate and *cis*-5,8,11,14,17-eicosapentaenoic acid in placentas. We suspected that DBP may inhibit the transfer of fatty acids from maternal serum and induce accumulation of fatty acids. Fetal development requires provision of fatty acids, especially essential fatty acids (Innis 2007) and disruption of fatty acid transfer may function against the fetal development.

CONCLUDING REMARKS

We here successfully developed malformed fetal mice model via intrauterine exposure to DBP during gestational days. The metabolomic profiling study of biological matrix including serum, placenta, and fetal brain tissue revealed a complex mechanism of teratogenesis induced by DBP including down-regulating of BCAAs in maternal serum that affects metabolism of neurotransmitters in fetal brain subsequently, disrupting of antioxidant system of the body and potentially inhibiting transport of fatty acids from dam to fetus. Combination of multiple sample matrices could provide a widened window to perceive the effect of DBP. As a result, characteristic metabolic variations associated with DBP induced developmental defects were observed including BCAAs and intermediate metabolites in TCA cycle in maternal serum, purine degradation products in the placenta and neurotransmitters in fetal brain tissue.

ABBREVIATIONS

DBP	Di-*n*-butyl phthalate
MVDA	Multivariate data analysis
GC/TOFMS	Gas chromatography time-of-flight mass spectrometry
NMR	Nuclear magnetic resonance
MS	Mass spectrometry
GC-MS or LC-MS	Gas chromatography or liquid chromatography coupled with mass spectrometry
gd	Gestation day
One-way ANOVA	One-way analysis of variance
PLS-DA	Partial least square-discriminant analysis
OPLS-DA	Orthogonal partial least square-discriminant analysis
VIP	Variable importance on project
TIC	Total ion current

BCAAs	Branched-chain amino acids
BCAT	Branched-chain aminotransferase
GABA	γ-amino-*n*-butyric acid
GSH	Glutathione

ACKNOWLEDGMENTS

This work was supported by National Basic Research Program of China (Grant #: 2007CB511905) and National comprehensive technology platforms for innovative drug R&D (Grant #: 2009ZX09301-007). The authors would especially like to thank all the study participants who contribute to this research.

CONFLICT OF INTEREST

No potential conflict of interest relevant to this article was reported.

REFERENCES

ATSDR. (1990). ATSDR-di-*n*-butylphthalate. Toxicological profile. Prepared by Life Systems Inc., under subcontract to: Clement Associates Inc., US Department of Health and Human Services, Public Health Service.

Bell, F. P. (1982). Effects of phthalate-esters on lipid-metabolism in various tissues, cells and organelles in mammals. *Environmental Health Perspectives, 45*, 41–50.

Bylesjo, M., Rantalainen, M., Cloarec, O., et al. (2006). OPLS discriminant analysis: Combining the strengths of PLS-DA and SIMCA classification. *Journal of Chemometrics, 20*(8–10), 341–351. www.umetrics.com.

Castellano, S., Casarosa, S., Sweatt, A. J., Hutson, S. M., & Bozzi, Y. (2007). Expression of cytosolic branched chain amino transferase (BCATc) mRNA in the developing mouse brain. *Gene Expression Patterns, 7*(4), 485–490.

Chan, P. K. L., & Meek, M. E. (1994). Di-*n*-butyl phthalate: Evaluation of risks to health from environmental exposure in Canada. *Journal of Environmental Science and Health, Part C: Environmental Carcinogenesis and Ecotoxicology Reviews, 12*(2), 257–268.

Chen, M. J., Su, M. M., Zhao, L. P., et al. (2006). Metabonomic study of aristolochic acid-induced nephrotoxicity in rats. *Journal of Proteome Research, 5*(4), 995–1002.

Dean, J. C. S., Hailey, H., Moore, S. J., et al. (2002). Long term health and neurodevelopment in children exposed to antiepileptic drugs before birth. *Journal of Medical Genetics, 39*(4), 251–259.

DeSesso, J. M., Scialli, A. R., & Holson, J. F. (1999). Apparent lability of neural tube closure in laboratory animals and humans. *American Journal of Medical Genetics, 87*(2), 143–162.

Ema, M., Amano, H., Itami, T., & Kawasaki, H. (1993). Teratogenic evaluation of di-*n*-butyl phthalate in rats. *Toxicology Letters, 69*(2), 197–203.

Fernie, A. R., Carrari, F., & Sweetlove, L. J. (2004). Respiratory metabolism: Glycolysis, the TCA cycle and mitochondrial electron transport. *Current Opinion in Plant Biology, 7*(3), 254–261.

Foster, P. M. D., Mylchreest, E., Gaido, K. W., & Sar, M. (2001). Effects of phthalate esters on the developing reproductive tract of male rats. *Human Reproduction Update, 7*(3), 231–235.

Gibney, M. J., Walsh, M., Brennan, L., et al. (2005). Metabolomics in human nutrition: opportunities and challenges. *American Journal of Clinical Nutrition, 82*(3), 497–503.

Gray, T. J. B., Rowland, I. R., Foster, P. M. D., & Gangolli, S. D. (1982). Species-differences in the testicular toxicity of phthalate-esters. *Toxicology Letters, 11*(1–2), 141–147.

Innis, S. M. (2007). Fatty acids and early human development. *Early Human Development, 83*(12), 761–766.

IPCS. (1997). *Environmental health criteria 189 di-n-butyl phthalate*. Geneva: Health Organization. ISBN 92-4-157189-6.

Kavlock, R., Boekelheide, K., Chapin, R., et al. (2002). NTP Center for the Evaluation of Risks to Human Reproduction: Phthalates expert panel report on the reproductive and developmental toxicity of di-*n*-butyl phthalate. *Reproductive Toxicology (Elmsford. NY), 16*(5), 489–527.

Kotch, L. E., Chen, S. Y., & Sulik, K. K. (1995). Ethanol-induced teratogenesis—Free-radical damage as a possible mechanism. *Teratology, 52*(3), 128–136.

Krebs, H. A. (1957). Control of metabolic processes. *Endeavour, 16*, 125–132.

Lauder, J. M. (1983). Hormonal and humoral influences on brain-development. *Psychoneuroendocrinology, 8*(2), 121–155.

Meister, A. (1974). Glutathione—Metabolism and function via gamma-glutamyl cycle. *Life Science, 15*(2), 177–190.

Meister, A. (1995). Glutathione metabolism. *Biothiols, Pt A, 251*, 3–7.

Melnick, R. L., & Schiller, C. M. (1982). Mitochondrial toxicity of phthalate-esters. *Environmental Health Perspectives, 45*, 51–56.

Ni, Y., Su, M. M., Lin, J. C., et al. (2008). Metabolic profiling reveals disorder of amino acid metabolism in four brain regions from a rat model of chronic unpredictable mild stress.

FEBS Letters, *582*(17), 2627–2636.

Nicholson, J. K., Lindon, J. C., & Holmes, E. (1999). 'Metabonomics': Understanding the metabolic responses of living systems to pathophysiological stimuli via multivariate statistical analysis of biological NMR spectroscopic data. *Xenobiotica, 29*(11), 1181–1189.

Pan, L., Qiu, Y., Chen, T., Lin, J., Chi, Y., Su, M., Zhao, A., & Jia, W. (2010). An optimized procedure for metabonomic analysis of rat liver tissue using gas chromatography/time-of-flight mass spectrometry. *Journal of Pharmaceutical and Biomedical Analysis, 52*, 589–596.

Pippenger, C. E. (2003). Pharmacology of neural tube defects. *Epilepsia, 44*, 24–32.

Prasanth, G. K., Divya, L. M., & Sadasivan, C. (2009). Effects of mono and di(*n*-butyl) phthalate on superoxide dismutase. *Toxicology, 262*(1), 38–42.

Premysl, M., Zdenka, S., & Miriam, S. (2005). Phthalates: Toxicology and food safety—A review. *Czech J Food Sci, 23*(6), 217–223.

Qiu, Y. P., Cai, G. X., Su, M. M., et al. (2009). Serum metabolite profiling of human colorectal cancer using GC-TOFMS and UPLC-QTOFMS. *Journal of Proteome Research, 8*(10), 4844–4850.

Qiu, Y. P., Cai, G. X., Su, M. M., et al. (2010). Urinary metabonomic study on colorectal cancer. *Journal of Proteome Research, 9*(3), 1627–1634.

Rull, R. P., Ritz, B., & Shaw, G. M. (2006). Neural tube defects and maternal residential proximity to agricultural pesticide applications. *American Journal of Epidemiology, 163*(8), 743–753.

Rustin, P. (2002). Mitochondria, from cell death to proliferation. *Nature Genetics, 30*(4), 352–353.

Saillenfait, A. M., Payan, J. P., Fabry, J. P., et al. (1998). Assessment of the developmental toxicity, metabolism, and placental transfer of di-*n*-butyl phthalate administered to pregnant rats. *Toxicological Sciences, 45*(2), 212–224.

Shiota, K., Chou, M. J., & Nishimura, H. (1980). Embryotoxic effects of di-2-ethylhexyl phthalate (DEHP) and di-*n*-butyl phthalate (DBP) in mice. *Environmental Research, 22*(1), 245–253.

Shiota, K., & Nishimura, H. (1982). Teratogenicity of di(2-ethylhexyl) phthalate (DEHP) and di-*n*-butyl phthalate (DBP) in mice. *Environmental Health Perspectives, 45*, 65–70.

Sugimoto, M., Kikuchi, S., Arita, M., et al. (2005). Large-scale prediction of cationic metabolite identity and migration time in capillary electrophoresis mass spectrometry using artificial neural networks. *Analytical Chemistry, 77*(1), 78–84.

Swan, S. H., Main, K. M., Liu, F., et al. (2005). Decrease in anogenital distance among male infants with prenatal phthalate exposure. *Environmental Health Perspectives, 113*(8), 1056–1061.

Tanaka, A., Matsumoto, A., & Yamaha, T. (1978). Biochemical studies on phthalic esters. III. Metabolism of dibutyl phthalate (DBP) in animals. *Toxicology, 9*(1–2), 109–123.

Um, S. Y., Chung, M. W., Kim, K. B., et al. (2009). Pattern recognition analysis for the prediction of adverse effects by nonsteroidal anti-inflammatory drugs using H-1 NMR-based metabolomics in rats. *Analytical Chemistry, 81*(12), 4734–4741.

Wang, X. Y., Su, M. M., Qiu, Y. P., et al. (2007). Metabolic regulatory network alterations in response to acute cold stress and ginsenoside intervention. *Journal of Proteome Research, 6*(9), 3449–3455.

Weckwerth, W., Loureiro, M. E., Wenzel, K., & Fiehn, O. (2004). Differential metabolic networks unravel the effects of silent plant phenotypes. *Proceedings of the National Academy of Sciences of the United States of America, 101*(20), 7809–7814.

Wellejus, A., Dalgaard, M., & Loft, S. (2002). Oxidative DNA damage in male wistar rats exposed to di-*n*-butyl phthalate. *Journal of Toxicology and Environmental Health—Part A, 65*(11), 813–824.

Wine, R. N., Li, L. H., Barnes, L. H., Gulati, D. K., & Chapin, R. E. (1997). Reproductive toxicity of di-*n*-butylphthalate in a continuous breeding protocol in Sprague–Dawley rats. *Environmental Health Perspectives, 105*(1), 102–107.

Wyde, M. E., Kirwan, S. E., Zhang, F., et al. (2005). Di-*n*-butyl phthalate activates constitutive androstane receptor and pregnane X receptor and enhances the expression of steroid-metabolizing enzymes in the liver of rat fetuses. *Toxicological Sciences, 86*(2), 281–290.

Yudkoff, M. (1997). Brain metabolism of branched-chain amino acids. *Glia, 21*(1), 92–98.